Process Simulation of Sulfuric Acid Recovery by Azeotropic Distillation: Vapor−Liquid Equilibria and Thermodynamic Modeling

ARTICLE *in* INDUSTRIAL & ENGINEERING CHEMISTRY RESEARCH · JULY 2014

Impact Factor: 2.59 · DOI: 10.1021/ie5013079

3 AUTHORS:

Geng Li
Chinese Academy of Sciences
5 PUBLICATIONS **20** CITATIONS
SEE PROFILE

Edouard Asselin
University of British Columbia - Vancouver
60 PUBLICATIONS **323** CITATIONS
SEE PROFILE

Zhibao Li
Chinese Academy of Sciences
67 PUBLICATIONS **602** CITATIONS
SEE PROFILE

I&EC research
Industrial & Engineering Chemistry Research

Article

pubs.acs.org/IECR

Process Simulation of Sulfuric Acid Recovery by Azeotropic Distillation: Vapor−Liquid Equilibria and Thermodynamic Modeling

Geng Li,[†] Edouard Asselin,[‡] and Zhibao Li*[,†]

[†]Key Laboratory of Green Process and Engineering, Institute of Process Engineering, Chinese Academy of Sciences, Beijing 100190, China

[‡]Department of Materials Engineering, The University of British Columbia, Vancouver, British Columbia V6T 1Z4, Canada

Supporting Information

ABSTRACT: For development of the new process for the recovery of dilute sulfuric acid by azeotropic distillation proposed in our earlier publication [Li et al., *Ind. Eng. Chem. Res.*, **2013**, *52*, 3481−3489], in this paper, the vapor−liquid equilibria (VLE) for the $FeSO_4 + H_2O$ and $H_2SO_4 + FeSO_4 + H_2O$ systems were first determined by the quasi-static ebulliometric method. The azeotropic temperatures of the $H_2SO_4 + H_2O$ + entrainer (cyclohexane and octane) systems were also measured. The corresponding electrolyte nonrandom two-liquid interaction parameters were obtained by regressing the experimental data with a maximum average absolute deviation of boiling points of 0.83 K. The model with newly obtained parameters was verified by comparing its prediction with the experimental azeotropic temperature for the $H_2SO_4 + FeSO_4 + H_2O + C_6H_{12}$ quaternary system. The temperature and sulfuric acid concentration ranges of the study were 305.9−396.9 K and 0−86.1 wt %, respectively. Following from the experimental results, semicontinuous distillation experiments for the sulfuric acid recovery were performed with cyclohexane as the entrainer. Equipped with the new parameters, Aspen Plus was adopted to carry out the process simulation for the recovery of dilute sulfuric acid by azeotropic distillation. The simulation results show that when cyclohexane was employed as the entrainer, the dilute sulfuric acid can be concentrated to 68% by a packed column containing 4 theoretical stages and with a reboiler temperature of only 361 K.

1. INTRODUCTION

The disposal of dilute sulfuric acid generated from sulfuric acid-consuming industrial sectors, such as TiO_2 production, steel manufacturing, and oil refining, has long been a serious problem.[1−6] There exist mainly two industrial-scale methods for the treatment of dilute sulfuric acid. One is to neutralize dilute sulfuric acid with lime to produce gypsum,[7,8] but the resultant gypsum causes a new environmental problem. The other is to enrich the dilute sulfuric acid by multistage evaporation,[9] which is quite energy-consuming. Other approaches[10−12] are not commonly used in industry.

In our most recent publication,[13] a new process for the recovery of dilute sulfuric acid by azeotropic distillation using butyl acetate as the entrainer was proposed. This process consists of three columns: the azeotropic distillation column, an acid column, and an entrainer recovery column. The dilute sulfuric acid and the recycled and makeup butyl acetate are fed into the middle of the azeotropic distillation column. The enriched sulfuric acid from the bottom is pumped to the acid column to recover butyl acetate and then sent for reuse. The overhead vapor from the distillation column is condensed and separated into two phases. The organic phase is returned to the distillation column, and the water phase is delivered to the entrainer recovery column to separate butyl acetate from water. However, later experimental studies showed that the butyl acetate tended to decompose over prolonged experimental durations. To further the development of this potential industrial-scale distillation process, different entrainers, such as cyclohexane and octane,[14,15] were identified as candidates and were tested. The effect of $FeSO_4$, which is the major impurity in the dilute sulfuric acid, also needs to be considered. To complement these studies, the vapor−liquid−liquid equilibria (VLLE) data and a thermodynamic model for the $H_2SO_4 + FeSO_4 + H_2O$ + cyclohexane (or octane) system are required.

The thermodynamic properties of sulfuric acid-containing systems have been extensively studied with various activity coefficient models over the years.[16−22] A chemical model based on the electrolyte nonrandom two-liquid (NRTL) model was built by Haghtalab et al.[23] to calculate the solubility of metal sulfates in sulfuric acid-containing systems, and an excellent agreement was achieved. Que et al.[24] developed a symmetric electrolyte NRTL model for the $H_2SO_4 + H_2O + SO_3$ system over the whole concentration range, and excellent matches between model correlations and available literature data were obtained. Recently, the electrolyte NRTL model was used by Park et al.[25] to successfully simulate the decomposition of sulfuric acid, and the results exhibited good accordance with experimental data.

The aim of this work was to establish a comprehensive thermodynamic model for the $H_2SO_4 + FeSO_4 + H_2O + C_6H_{12}$ system and to carry out the associated experimental study for the purposes of validation. A simulation of the azeotropic distillation process could then be performed with reasonable confidence. Specifically, the boiling points were determined by

Received: March 28, 2014
Revised: June 14, 2014
Accepted: June 25, 2014
Published: June 25, 2014

the ebulliometric method for the $FeSO_4 + H_2O$ and $H_2SO_4 + FeSO_4 + H_2O$ systems. Then, the azeotropic temperatures of $H_2SO_4 + H_2O + C_6H_{12}$, $H_2SO_4 + H_2O + C_8H_{12}$, and $H_2SO_4 + FeSO_4 + H_2O + C_6H_{12}$ systems were investigated. A thermodynamic model for the system was developed on the basis of the electrolyte NRTL model and the model parameters for the pairs $H_2O-[Fe]^{2+}:[SO_4]^{2-}$, $[H_3O]^+:[SO_4]^{2-}-[Fe]^{2+}:[SO_4]^{2-}$, $[H_3O]^+:[HSO_4]^--[Fe]^{2+}:[HSO_4]^-$, $C_6H_{12}-[H_3O]^+:[HSO_4]^-$, $C_6H_{12}-[H_3O]^+:[SO_4]^{2-}$, $C_8H_{18}-[H_3O]^+:[HSO_4]^-$, and $C_8H_{18}-[H_3O]^+:[SO_4]^{2-}$ were regressed from the experimental data. On the basis of the new thermodynamic model, the process simulation was performed using Aspen Plus. The experimental data, the model with new parameters, and the process simulation results provide basic knowledge for the development of an industrial-scale process for the recovery of dilute sulfuric acid by azeotropic distillation.

2. EXPERIMENTAL SECTION

2.1. Experimental Materials. The sulfuric acid was supplied by Beijing Chemical Plant with mass fraction purity of 0.95−0.98. The main impurity is water, while other impurities, namely salts, are less than 0.01 wt %. The ferrous sulfate and the cyclohexane were supplied by Xilong Chemical Co., Ltd. with mass fraction purities of 0.994 and 0.990, respectively. The octane was supplied by Sinapharm Chemical Reagent Co., Ltd. with minimum mass fraction purity of 0.98. All were analytical grade and used without further purification. The deionized water was produced in a local laboratory.

2.2. Experimental Apparatus. *2.2.1. Boiling Point Measurement.* The boiling points of the systems were determined by the quasi-static ebulliometric method. The detailed description of the apparatus can be found in our earlier publications.[13,26]

2.2.2. Distillation Experiments. Azeotropic distillation experiments were performed using the experimental distillation column shown in Figure 1. The apparatus consists of a reboiler flask with a volume of 2 L, a 50 mm diameter column packed with glass helix rings (Φ10 × 4 mm), a condenser with decanter at the bottom, and a heating jacket with maximum heating power of 0.5 kW. The condenser was cooled by tap water.

2.3. Experimental Procedure. *2.3.1. Boiling Point Measurement.* The experimental procedure was exactly the same as that followed in our previous work.[13] The system pressures of (5, 10, 15, 20, 30, 60, 90, and 101.3) kPa were obtained by controlling the water temperature to (306.09, 319.03, 327.20, 333.29, 342.35, 359.15, 369.85, and 373.15) K, respectively, according to the Antoine equation. The Antoine equation constants[27] for water are listed in Table S1 of Supporting Information.

2.3.2. Semicontinuous Distillation. The procedure of the distillation experiments was as follows: an adequate amount (120 mL) of entrainer (cyclohexane or octane) was first charged into the flask at the bottom of the distillation column. The column was operated at full reflux until the temperature and the reflux were stable. Then, the sulfuric acid with a concentration of 20% (wt %) was fed through a nozzle near the top of the column by a peristaltic pump. The overhead vapor from the column was condensed and separated into two phases in the decanter. The upper organic phase was returned back to the top of the distillation column as reflux, and the water phase was removed from the bottom of the decanter. After the distillation column had reached stable operation, the sulfuric acid concentration in the flask was calculated by the amount of sulfuric acid pumped in and the amount of water extracted out for the same time period. The heating power and the speed of the pump were carefully adjusted until the expected sulfuric acid concentration (>60 wt %) was obtained in the flask. The heating power, speed of input, and the temperature in the flask were then recorded.

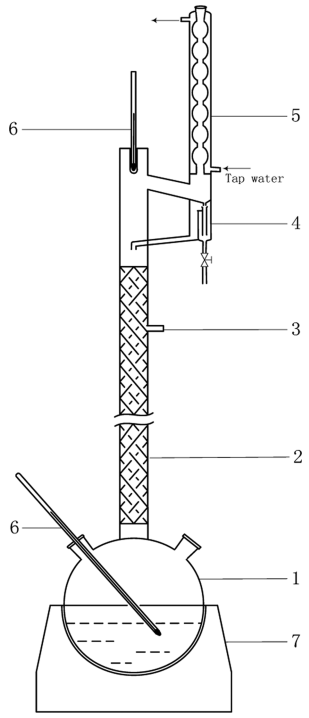

Figure 1. Schematic drawing of the distillation experiment apparatus: (1) flask, (2) column, (3) feeding nozzle, (4) decanter, (5) condenser, (6) microthermometer, and (7) heating jacket.

3. THERMODYNAMIC MODELING

3.1. Vapor−Liquid Equilibrium. A general vapor−liquid equilibrium relationship can be expressed as[28]

$$Py_i\varphi_i = x_i\gamma_i P_i^S \varphi_i^S \theta_i^S \quad (1)$$

Where P_i^S is the vapor pressure of pure component i at the system temperature T, calculated by the Antoine equation using the parameters[27] listed in Table S1 of Supporting Information.

The Poynting pressure correction θ_i^S and fugacity coefficient φ_i and φ_i^S could be reasonably assumed to be unity at low equilibrium pressures, and then eq 1 can be simplified to[28]

$$Py_i = x_i\gamma_i P_i^S \quad (2)$$

3.2. Dissociation Reactions. Proper description of chemical reactions is required for the thermodynamic modeling of electrolyte solutions. For $H_2SO_4 + FeSO_4 + H_2O$ + entrainer systems, the electrolyte NRTL model embedded in Aspen Plus (Version 7.2) was selected, and the main dissociation reactions are summarized in eqs 3−6.

$$H_2SO_4 + H_2O \leftrightarrow HSO_4^- + H_3O^+ \quad (3)$$

$$HSO_4^- + H_2O \leftrightarrow SO_4^{2-} + H_3O^+ \quad (4)$$

$$FeSO_4 \leftrightarrow SO_4^{2-} + Fe^{2+} \quad (5)$$

$$2H_2O \leftrightarrow H_3O^+ + OH^- \quad (6)$$

dx.doi.org/10.1021/ie5013079 | Ind. Eng. Chem. Res. 2014, 53, 11794−11804

3.3. Activity Coefficient Model. The activity coefficient is a thermodynamic state function, which accounts for nonideality (excess properties) of an electrolyte solution, and is derived from the excess Gibbs free energy of the solution:

$$\ln \gamma_i = \left(\frac{\partial (n_{\text{total}} G^{\text{E}}/RT)}{\partial n_i} \right)_{T,P,n_j} \tag{7}$$

The electrolyte NRTL model consists of two contributions:[29] one from long-range ion−ion interactions represented by the Pitzer−Debye−Hückel model[31] and Born equation, and one from local interaction described by the nonrandom two-liquid theory.[30] The excess Gibbs energy model is expressed as follows:

$$\frac{G_m^{*\text{E}}}{RT} = \frac{G_m^{*\text{E,PDH}}}{RT} + \frac{G_m^{*\text{E,Born}}}{RT} + \frac{G_m^{*\text{E,lc}}}{RT} \tag{8}$$

which leads to

$$\ln \gamma_i^* = \ln \gamma_i^{*\text{PDH}} + \ln \gamma_i^{*\text{Born}} + \ln \gamma_i^{*\text{lc}} \tag{9}$$

The expression for the Pitzer−Debye−Hückel equation is given by[29]

$$\ln \gamma_i^{*\text{PDH}} = -\left(\frac{1000}{M_{\text{B}}} \right)^{1/2} A \left[\left(\frac{2Z_i^2}{\rho} \right) \ln(1 + \rho I_x^{1/2}) + \frac{Z_i^2 I_x^{1/2} - 2I_x^{3/2}}{1 + \rho I_x^{1/2}} \right] \tag{10}$$

The expression for the activity coefficient of the Born equation is[29]

$$\ln \gamma_i^{*\text{Born}} = \frac{Q_e^2}{2kT} \left(\frac{1}{\varepsilon} - \frac{1}{\varepsilon_{\text{w}}} \right) \frac{Z_i^2}{r_i} 10^{-2} \tag{11}$$

In a multicomponent solution, the local composition activity coefficient equations for cation, anion, and molecular components are given by the following equations:

$$\frac{1}{Z_c} \ln \gamma_c^{\text{lc}} = \sum_{a'} \left(\frac{X_{a'}}{\sum_{a''} X_{a''}} \right) \frac{\sum_k X_k G_{kc,a'c} \tau_{kc,a'c}}{\sum_k X_k G_{kc,a'c}} + \sum_{B'} \frac{X_B G_{cB}}{\sum_k X_k G_{kB}} \left(\tau_{cB} - \frac{\sum_k X_k G_{kB} \tau_{kB}}{\sum_k X_k G_{kB}} \right) + \sum_a \sum_{c'} \left(\frac{X_{c'}}{\sum_{c''} X_{c''}} \right) \frac{X_a G_{ca,c'a}}{\sum_k X_k G_{ka,c'a}} \left(\tau_{ca,c'a} - \frac{\sum_k X_k G_{ka,c'a} \tau_{ka,c'a}}{\sum_k X_k G_{ka,c'a}} \right) \tag{12}$$

$$\frac{1}{Z_a} \ln \gamma_a^{\text{lc}} = \sum_{c'} \left(\frac{X_{c'}}{\sum_{c''} X_{c''}} \right) \frac{\sum_k X_k G_{ka,c'a} \tau_{ka,c'a}}{\sum_k X_k G_{kc,c'a}} + \sum_B \frac{X_B G_{aB}}{\sum_k X_k G_{kB}} \left(\tau_{aB} - \frac{\sum_k X_k G_{kB} \tau_{kB}}{\sum_k X_k G_{kB}} \right) + \sum_c \sum_{a'} \left(\frac{X_{a'}}{\sum_{a''} X_{a''}} \right) \frac{X_c G_{ac,a'c}}{\sum_k X_k G_{kc,a'c}} \times \left(\tau_{ac,a'c} - \frac{\sum_k X_k G_{kc,a'c} \tau_{kc,a'c}}{\sum_k X_k G_{kc,a'c}} \right) \tag{13}$$

$$\ln \gamma_B^{\text{lc}} = \frac{\sum_j X_j G_{jB} \tau_{jB}}{\sum_k X_k G_{kB}} + \sum_{B'} \frac{X_{B'} G_{BB'}}{\sum_k X_k G_{kB'}} \left(\tau_{BB'} - \frac{\sum_k X_k G_{kB'} \tau_{kB'}}{\sum_k X_k G_{kB'}} \right) + \sum_c \sum_{a'} \left(\frac{X_a}{\sum_{a''} X_{a''}} \right) \frac{X_c G_{Bc,a'c}}{\sum_k X_k G_{kc,a'c}} \left(\tau_{Bc,a'c} - \frac{\sum_k X_k G_{kc,a'c} \tau_{kc,a'c}}{\sum_k X_k G_{kc,a'c}} \right) + \sum_a \sum_{c'} \left(\frac{X_{c'}}{\sum_{c''} X_{c''}} \right) \frac{X_a G_{Ba,c'a}}{\sum_k X_k G_{ka,c'a}} \left(\tau_{Bc,c'a} - \frac{\sum_k X_k G_{ka,c'a} \tau_{ka,c'a}}{\sum_k X_k G_{ka,c'a}} \right) \tag{14}$$

where

$$\ln G_{ka,c'a} = -\tau_{ka,c'a} \alpha \tag{15}$$

$$\tau_{cB} = \tau_{aB} = \tau_{ca,B}; \quad \tau_{Bc} = \tau_{Ba} = \tau_{B,ca}; \quad \tau_{Bc,ac} = \tau_{Ba,ca} = \tau_{B,ca} \tag{16}$$

and where $X_j = x_j Z_j$ is the effective mole fraction of species j.

Normally, the value of α is 0.2 for molecule−electrolyte and electrolyte−electrolyte pairs.[32] The energy parameters τ can be assumed to be temperature-dependent as follows:[29]

$$\tau_{ca,B} = C_{ca,B} + \frac{D_{ca,B}}{T} + E_{ca,B} \left[\frac{(T^{\text{ref}} - T)}{T} + \ln \left(\frac{T}{T^{\text{ref}}} \right) \right] \tag{17}$$

where ca means electrolyte (cation−anion). T^{ref} is reference temperature (273.15 K), and C_{ij}, D_{ij}, E_{ij}, and α (=0.2 in this work) are adjustable parameters.

The Data Regression System (DRS) incorporated in Aspen Plus (Version 7.2) was employed in the correlation, and the following objective function was minimized to obtain the optimal parameter values by fitting the experimental boiling point data on the basis of the maximum likelihood principle:[33]

$$F_{\text{OB}} = \sum_{n=1}^{\text{NDG}} w_n \sum_{i=1} \left[\left(\frac{T_i^{\text{exp}} - T_i^{\text{cal}}}{\sigma_T} \right)^2 + \left(\frac{p_i^{\text{exp}} - p_i^{\text{cal}}}{\sigma_p} \right)^2 + \left(\frac{z_i^{\text{exp}} - z_i^{\text{cal}}}{\sigma_z} \right)^2 \right] \tag{18}$$

where σ is standard deviation (0.1 K for temperature, 0.1% for pressure, and 1% for the feed composition z). w is the weight factor (w_n = 1 in this work), and n represents data group; z is the feed composition. NDG, exp, and cal mean number of data group, experimental data, and calculated result, respectively.

4. RESULTS AND DISCUSSION

4.1. VLE and VLLE Measurement. *4.1.1. Boiling Point Measurement.* The boiling point data were determined at (5, 10, 15, and 20) kPa for the $FeSO_4 + H_2O$ binary system and at (30, 60, 90, and 101.3) kPa for the $H_2SO_4 + FeSO_4 + H_2O$ ternary system. They are tabulated in Tables S2 and S3 of Supporting Information and illustrated in Figures 2 and 3, respectively. For the $FeSO_4 + H_2O$ system, the boiling point increases slightly with increasing concentration of ferrous sulfate (m_1) in the concentration range investigated. The boiling point increases only by 0.66 K at 20 kPa when the ferrous sulfate concentration increases from 0 to 1.75 mol/kg. As for the $H_2SO_4 + FeSO_4 + H_2O$ system, the measurement of VLE was carried out at fixed sulfuric acid/water ratios, namely, x_1/x_3 = 0.0204, x_1/x_3 = 0.0459, x_1/x_3 = 0.0787, and x_1/x_3 =

dx.doi.org/10.1021/ie5013079 | Ind. Eng. Chem. Res. 2014, 53, 11794−11804

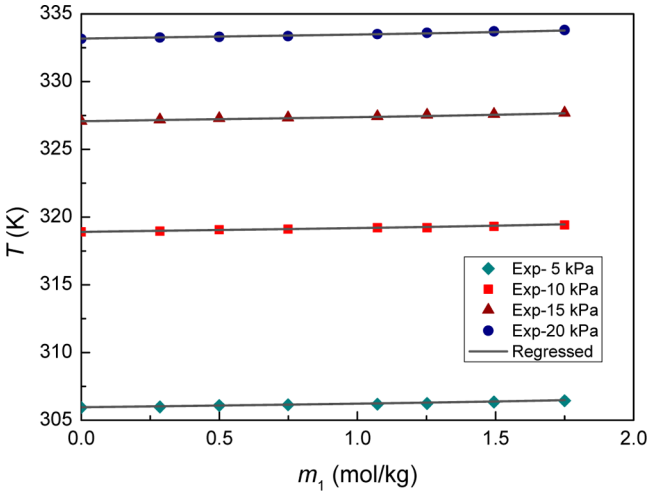

Figure 2. Boiling points of the $FeSO_4$ (1) + H_2O (2) binary system.

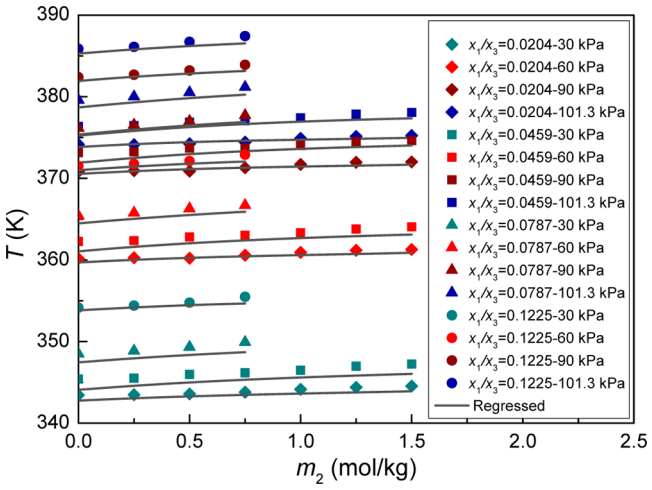

Figure 3. Boiling points of the H_2SO_4 (1) + $FeSO_4$ (2) + H_2O (3) ternary system.

0.1225. It can be seen from Figure 3 that the boiling point also increases when the ratio of sulfuric acid/water increases.

4.1.2. Azeotropic Temperature Measurement. The azeotropic temperatures were also determined at (30, 60, 90, and 101.3) kPa for the following heterogeneous systems: H_2SO_4 + H_2O + C_6H_{12}, H_2SO_4 + H_2O + C_8H_{18}, and H_2SO_4 + $FeSO_4$ + H_2O + C_6H_{12}. These results are given in Tables 1−3 and depicted in Figures 4−6, respectively. Figure 4 demonstrates that the azeotropic temperature increases as the concentration of sulfuric acid increases. But when the concentration of sulfuric acid is higher than 80%, the azeotropic temperature is almost invariant and close to the boiling point of pure cyclohexane (e.g., 353.9 K at 101.3 kPa). A similar phenomenon occurred for the H_2SO_4 + H_2O + C_8H_{18} system, as shown in Figure 5. As for the H_2SO_4 + $FeSO_4$ + H_2O + C_6H_{12} quaternary system, the azeotropic temperature increases slightly with increasing concentration of ferrous sulfate at fixed ratios of sulfuric acid/water, while it also increases as the ratio of sulfuric acid/water increases at fixed $FeSO_4$ concentration.

4.2. Evaluation of the Existing Model. The accuracy of the existing model of Aspen Plus in predicting the azeotropic temperatures of the H_2SO_4 + H_2O + C_6H_{12} (C_8H_{18}) systems was evaluated by comparing the predictions of Aspen Plus with the experimental data. It can be seen from Figure 4 that the model with default parameters cannot describe the azeotropic temperature of the H_2SO_4 + H_2O + C_6H_{12} system when the sulfuric acid concentration is over 20% (wt %), and very large deviation for temperature of 50 K is observed when the sulfuric acid concentration is 60%. Figure 5 provides a comparison between the calculated value and the experimental data for the H_2SO_4 + H_2O + C_8H_{18} system. A significant deviation is also noticed when the sulfuric acid concentration is larger than 30%.

4.3. Model Parameterization. In order to improve the capacity of Aspen Plus to predict thermodynamic equilibria for these systems, new electrolyte NRTL model parameters were regressed from the experimental data presented above. The resulting parameters are listed in Table 4.

The interaction parameters for pairs H_2O−Fe^{2+}:SO_4^{2-} and Fe^{2+}:SO_4^{2-}−H_2O were obtained by correlating the experimental boiling point data of the $FeSO_4$ + H_2O binary system. The fitted results are compared with the experimental data in Figure 2. A good agreement is achieved with an overall maximum absolute deviation (MAD) for temperature of 0.09 K and an overall average absolute deviation (AAD) for temperature of 0.04 K, as listed in Table 5. The interaction parameters for pairs Fe^{2+}:HSO_4^-−H_3O^+:HSO_4^-, H_3O^+:HSO_4^-−Fe^{2+}:HSO_4^-, Fe^{2+}:SO_4^{2-}−H_3O^+:SO_4^{2-}, and H_3O^+:SO_4^{2-}−Fe^{2+}:SO_4^{2-} were regressed from the experimental data for the H_2SO_4 + $FeSO_4$ + H_2O ternary system. The calculated results with the newly obtained parameters, as depicted in Figure 3, are in accordance with the experimental data with a MAD (T) of 1.32 K and an AAD (T) of 0.59 K.

Table 1. Azeotropic Temperatures of the H_2SO_4 (1) + H_2O (2) + C_6H_{12} (3) Ternary System

				T (K)			
x_1	x_2	x_3	wt % (1)	p = 30 kPa	p = 60 kPa	p = 90 kPa	p = 101.3 kPa
0.0000	0.9000	0.1000	0.00	311.55	328.30	339.02	342.62
0.0180	0.9261	0.0559	9.59	311.60	328.40	339.12	342.72
0.0416	0.8877	0.0708	20.31	312.16	329.21	339.93	343.43
0.0641	0.8628	0.0730	28.81	312.56	329.61	340.44	343.89
0.1001	0.8194	0.0805	39.94	314.23	331.48	342.47	346.22
0.1454	0.7671	0.0876	50.78	315.91	333.96	345.86	349.37
0.1994	0.7042	0.0964	60.66	316.82	335.27	347.39	351.10
0.2640	0.6280	0.1080	69.59	317.68	336.59	348.96	352.67
0.3921	0.4625	0.1454	82.19	318.04	337.20	349.88	353.79
0.4266	0.4421	0.1313	84.01	318.04	337.25	349.98	353.84
0.4398	0.3859	0.1743	86.12	318.09	337.30	349.98	353.84

dx.doi.org/10.1021/ie5013079 | Ind. Eng. Chem. Res. 2014, 53, 11794−11804

Table 2. Azeotropic Temperatures of the H_2SO_4 (1) + H_2O (2) + C_8H_{18} (3) Ternary System

				T (K)			
x_1	x_2	x_3	wt % (1)	p = 30 kPa	p = 60 kPa	p = 90 kPa	p = 101.3 kPa
0.0000	0.9476	0.0524	0.0000	332.46	348.91	359.08	362.23
0.0190	0.9301	0.0509	10.0000	333.26	349.42	359.84	363.25
0.0417	0.9088	0.0494	19.9999	334.48	350.94	361.32	364.58
0.0691	0.8779	0.0530	29.9999	335.49	351.75	362.64	365.70
0.1032	0.8428	0.0540	39.9999	338.57	355.51	366.11	369.78
0.1463	0.7964	0.0573	50.0000	342.32	359.64	371.21	374.62
0.2036	0.7388	0.0576	60.0001	348.30	366.11	378.17	381.82
0.2803	0.6541	0.0656	70.0000	355.01	374.01	386.86	390.98
0.3963	0.5394	0.0643	79.9999	358.06	378.37	392.51	396.90

Table 3. Azeotropic Temperatures of the H_2SO_4 (1) + $FeSO_4$ (2) + H_2O (3) + C_6H_{12} (4) Quaternary System

					T (K)			
x_1	x_2	x_3	x_4	m_2 (mol·kg^{-1})	p = 30 kPa	p = 60 kPa	p = 90 kPa	p = 101.3 kPa
				x_1/x_3 = 0.0180				
0.0163	0.0000	0.9041	0.0796	0.0000	311.67	328.97	339.28	343.08
0.0164	0.0082	0.9112	0.0642	0.5000	311.67	328.82	339.28	342.93
0.0163	0.0163	0.9061	0.0613	1.0000	311.97	328.92	339.69	343.23
0.0161	0.0242	0.8939	0.0659	1.5000	312.17	329.23	339.99	343.53
				x_1/x_3 = 0.0459				
0.0419	0.0000	0.9130	0.0451	0.0000	312.28	328.87	339.94	343.69
0.0407	0.0080	0.8861	0.0652	0.5000	312.63	329.38	340.19	343.84
0.0412	0.0162	0.8980	0.0445	1.0000	312.78	329.58	340.50	344.04
0.0406	0.0239	0.8841	0.0514	1.5000	312.88	329.78	340.70	344.19
				x_1/x_3 = 0.0787				
0.0689	0.0000	0.8758	0.0552	0.0000	312.88	329.93	340.60	343.94
0.0690	0.0079	0.8764	0.0468	0.5000	313.59	330.39	341.31	344.75
				x_1/x_3 = 0.1225				
0.1022	0.0000	0.8347	0.0631	0.0000	313.69	330.69	342.12	345.71
0.1011	0.0074	0.8253	0.0662	0.5000	314.00	331.19	342.32	345.87

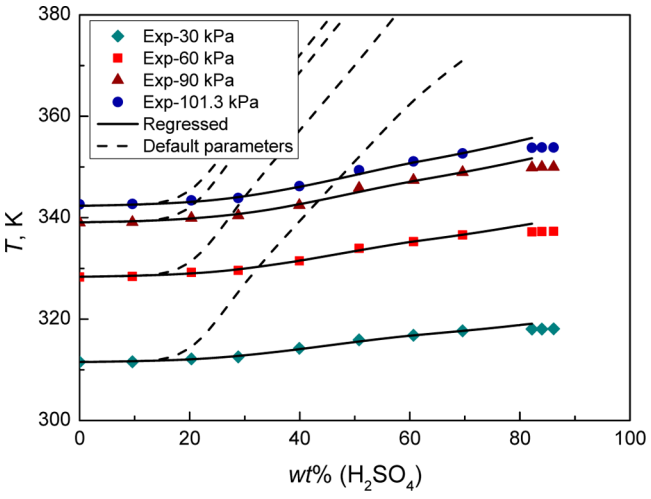

Figure 4. Azeotropic temperatures of the H_2SO_4 + H_2O + C_6H_{12} ternary system.

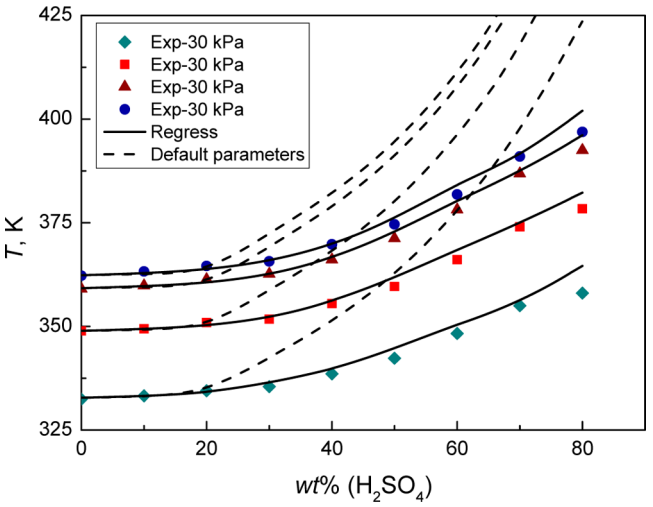

Figure 5. Azeotropic temperatures of the H_2SO_4 + H_2O + C_8H_{18} ternary system.

The parameters for pairs C_6H_{12}–H_3O^+:HSO_4^-, H_3O^+:HSO_4^-–C_6H_{12}, C_6H_{12}–H_3O^+:SO_4^{2-}, and H_3O^+:SO_4^{2-}–C_6H_{12} were regressed directly from the experimental azeotropic temperature data of the H_2SO_4 + H_2O + C_6H_{12} ternary heterogeneous system. Figure 4 demonstrates that the obtained parameters can adequately describe the azeotropic temperature when the sulfuric acid concentration is no more than 70% (wt %) with the MAD (T) and the AAD (T) of only 0.78 and 0.18 K, respectively. The parameters for pairs C_8H_{18}–H_3O^+:HSO_4^-, H_3O^+:HSO_4^-–C_8H_{18}, C_8H_{18}–H_3O^+:SO_4^{2-}, and H_3O^+:SO_4^{2-}–C_8H_{18} were obtained directly from the azeotropic temperature data of the H_2SO_4 + H_2O + C_8H_{18} ternary system. It can be seen in Figure 5 that the regression fitted the experimental data well when the sulfuric acid concentration was less than 70% with a MAD (T) of 2.65

dx.doi.org/10.1021/ie5013079 | Ind. Eng. Chem. Res. 2014, 53, 11794–11804

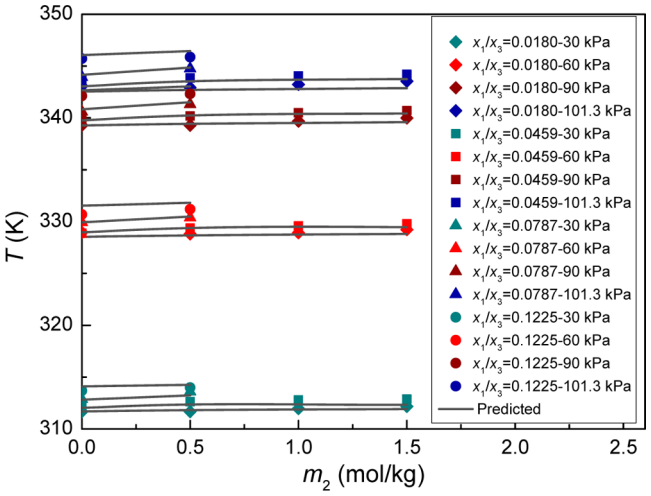

Figure 6. Azeotropic temperatures of the H_2SO_4 + $FeSO_4$ + H_2O + C_6H_{12} quaternary system.

K and an AAD (T) of 0.83 K, as listed in Table 6. Compared with the default parameters, the newly obtained parameters evidently improve the accuracy of the Aspen Plus calculation for these heterogeneous systems.

When the boiling point and the azeotropic temperature of the above-mentioned binary and ternary systems were successfully modeled, a private parameter data bank was built in which the newly obtained electrolyte NRTL model parameters were added, as shown in Table 4. We then proceeded to test the new model in the case of the H_2SO_4 + $FeSO_4$ + H_2O + C_6H_{12} quaternary heterogeneous system. The prediction of the azeotropic temperature of the quaternary system was carried out using a three-phase flash model incorporated in Aspen Plus, which can perform rigorous VLL equilibria calculations. Figure 6 shows that a good agreement is obtained between the experimental azeotropic temperature data and prediction for the quaternary system with a MAD (T) of 0.84 K and an AAD (T) of 0.30 K, as listed in Table 7. The model with new parameters is sufficiently accurate to be used in our simulations of the azeotropic distillation of dilute sulfuric acid.

Table 5. Deviations between the Experimental and Regressed Boiling Point (ΔT) for the H_2SO_4 + $FeSO_4$ + H_2O and $FeSO_4$ + H_2O Systems[a]

	H_2SO_4 + $FeSO_4$ + H_2O			$FeSO_4$ + H_2O	
p (kPa)	$\lvert\Delta T\rvert_{av}$ (K)	$\lvert\Delta T\rvert_{max}$ (K)	p (kPa)	$\lvert\Delta T\rvert_{av}$ (K)	$\lvert\Delta T\rvert_{max}$ (K)
30	0.75	1.32	5	0.25	0.55
60	0.59	1.19	10	0.27	0.84
90	0.49	1.22	15	0.26	0.71
101.3	0.52	1.14	20	0.40	0.66
overall	0.59	1.32	overall	0.30	0.84

[a] $\lvert\Delta T\rvert = \lvert T_{cal} - T_{exp}\rvert$; $\lvert\Delta T\rvert_{av} = (\Sigma_{i=1}^{n}\lvert\Delta T\rvert_k)/n$, where n is the number of data points

Table 6. Deviations between the Experimental and Regressed Azeotropic Temperatures (ΔT) for the H_2SO_4 + H_2O + Entrainer Systems[a] (Sulfuric Acid Concentration, 0−70%)

	H_2SO_4 + H_2O + C_6H_{12}		H_2SO_4 + H_2O + C_8H_{18}	
p (kPa)	$\lvert\Delta T\rvert_{av}$ (K)	$\lvert\Delta T\rvert_{max}$ (K)	$\lvert\Delta T\rvert_{av}$ (K)	$\lvert\Delta T\rvert_{max}$ (K)
30	0.11	0.28	1.01	2.36
60	0.14	0.39	0.87	2.38
90	0.21	0.78	0.72	2.27
101.3	0.27	0.78	0.72	2.65
overall	0.18	0.78	0.83	2.65

[a] $\lvert\Delta T\rvert = \lvert T_{cal} - T_{exp}\rvert$; $\lvert\Delta T\rvert_{av} = (\Sigma_{i=1}^{n}\lvert\Delta T\rvert_k)/n$, where n is the number of data points

Table 4. Electrolyte NRTL Parameters[a] for the H_2SO_4 + $FeSO_4$ + H_2O + Entrainer Systems

no.	component i	component j	C	D	E	α_{ij}
1	H_2O	Fe^{2+}:SO_4^{2-}	8.0443			0.20
2	Fe^{2+}:SO_4^{2-}	H_2O	−4.0058			0.20
3	Fe^{2+}:HSO_4^-	H_3O^+:HSO_4^-	9.9716	−274.37	−4.8668	0.20
4	H_3O^+:HSO_4^-	Fe^{2+}:HSO_4^-	8.8399	−93.018	−0.785 12	0.20
5	Fe^{2+}:SO_4^{2-}	H_3O^+:SO_4^{2-}	7.4457	−285.83	0.249 60	0.20
6	H_3O^+:SO_4^{2-}	Fe^{2+}:SO_4^{2-}	−2.6811	−231.80	−0.951 32	0.20
7	C_6H_{12}	H_3O^+: HSO_4^-	1.8482	1714.9	51.580	0.20
8	H_3O^+:HSO_4^-	C_6H_{12}	−0.027 91	−318.60	9.0661	0.20
9	C_6H_{12}	H_3O^+:SO_4^{2-}	2.8165			0.20
10	H_3O^+:SO_4^{2-}	C_6H_{12}	−3.1165			0.20
11	C_8H_{18}	H_3O^+: HSO_4^-	−7.7440	4989.1	−61.207	0.20
12	H_3O^+: HSO_4^-	C_8H_{18}	−16.304	4793.8	114.22	0.20
13	C_8H_{18}	H_3O^+:SO_4^{2-}	15.716			0.20
14	H_3O^+:SO_4^{2-}	C_8H_{18}	−5.2558			0.20
15	H_2O	H_3O^+:HSO_4^-	6.3620	1958.2	−4.5990	0.20
16	H_3O^+:HSO_4^-	H_2O	−3.7490	−583.20	4.4720	0.20
17	H_2O	H_3O^+:SO_4^{2-}	8.0000	0		0.20
18	H_3O^+:SO_4^{2-}	H_2O	−4.0000	0		0.20
19	H_2O	C_6H_{12}	13.143	−1067.0		0.20
20	C_6H_{12}	H_2O	−10.459	4954.9		0.20
21	H_2O	C_8H_{18}	1.2166	2997.7		0.20
22	C_8H_{18}	H_2O	−12.035	5381.4		0.20

[a] Parameters (1−14) obtained in this work, (15−18) from Aspen Plus ENRTL data bank, and (19−22) from Aspen Plus LLE data bank.

dx.doi.org/10.1021/ie5013079 | Ind. Eng. Chem. Res. 2014, 53, 11794−11804

Table 7. Deviations between the Experimental and Predicted Azeotropic Temperatures (ΔT) for the H_2SO_4 + $FeSO_4$ + H_2O + C_6H_{12} System[a]

	H_2SO_4 + $FeSO_4$ + H_2O + C_6H_{12}	
p (kPa)	$\lvert\Delta T\rvert_{av}$ (K)	$\lvert\Delta T\rvert_{max}$ (K)
30	0.25	0.55
60	0.27	0.84
90	0.26	0.71
101.3	0.40	0.66
overall	0.30	0.84

[a] $\lvert\Delta T\rvert = \lvert T_{cal} - T_{exp}\rvert$; $\lvert\Delta T\rvert_{av} = (\Sigma_{i=1}^{n}\lvert\Delta T\rvert_k)/n$, where n is the number of data points

4.4. Speciation. The new model was also used to analyze the temperature and concentration effect on the speciation in the H_2SO_4 + $FeSO_4$ + H_2O system.

4.4.1. Temperature Effect. The fractions of sulfuric acid species (H_2SO_4, HSO_4^-, and SO_4^{2-}) for the ternary system at 101.3 kPa ($m_{H_2SO_4}$ = 1 mol/kg; m_{FeSO_4} = 1 mol/kg) as a function of temperature are shown in Figure 7. It can be observed that the fraction of HSO_4^- increases as temperature increases, indicating a decrease in the degree of ion dissociation. Simultaneously, the concentration of SO_4^{2-} decreases with increasing temperature. The percentages of HSO_4^- and SO_4^{2-} are 40.23% and 59.77%, respectively, at 290 K, but 75.32% and 24.68%, respectively, at 370 K. The proportion of neutral species H_2SO_4 in the system is nearly zero throughout the entire temperature range studied.

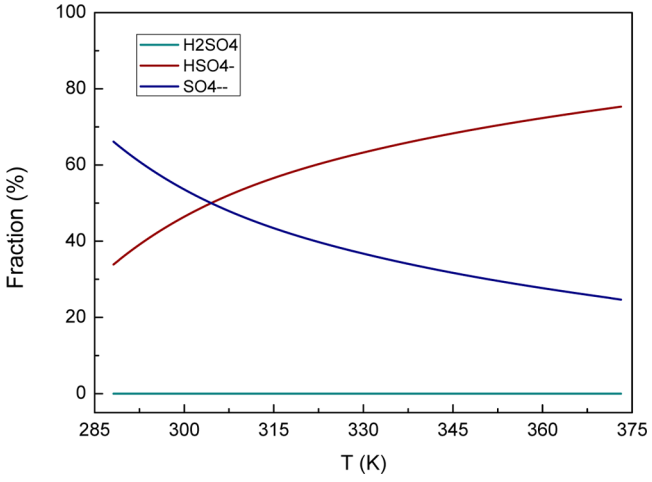

Figure 7. Speciation as a function of temperature for the H_2SO_4 + $FeSO_4$ + H_2O system at 101.3 kPa ($m_{H_2SO_4}$ = 1 mol/kg; m_{FeSO_4} = 1 mol/kg).

4.4.2. Concentration Effect. The relative concentrations of sulfate species for the system at 298 and 373 K at 101.3 kPa (m_{FeSO_4} = 1 mol/kg) as a function of sulfuric acid concentration are illustrated in Figure 8. It is obvious that the proportion of HSO_4^- first decreases sharply with sulfuric acid to a minimum, then decreases slightly after passing a maximum, while the fraction of SO_4^{2-} first increases sharply to a maximum, then increases slightly after passing a minimum at 298 K. The fraction of HSO_4^- consistently decreases, while the fraction of SO_4^{2-} continuously increases at 373 K. The content of the H_2SO_4 molecule in the system is almost equal to zero at both temperatures throughout the sulfuric acid concentration range investigated.

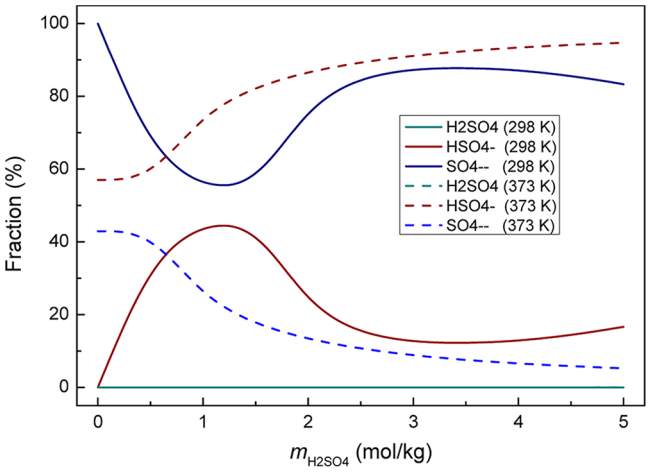

Figure 8. Speciation as a function of sulfuric acid concentration for the H_2SO_4 + $FeSO_4$ + H_2O system at 298 and 373 K at 101.3 kPa (m_{FeSO_4} = 1 mol/kg).

4.5. Azeotropic Distillation. Semicontinuous experimental scale azeotropic distillation was carried out using the apparatus depicted in Figure 1. The operating conditions that resulted in successful enrichment of the sulfuric acid from 20% to 60% are tabulated in Table 8. We can see that when octane is used as the entrainer, the temperature at the bottom of the column is about 410 K. This temperature is nearly the same as the boiling point of sulfuric acid with a concentration of 60%, and still high grade heating steam is required. But when cyclohexane is employed as the entrainer, the bottom temperature of the column is only about 370 K, which is about 40 K lower than the boiling temperature of a 60% sulfuric acid. This indicates that a lower quality heating steam is required, and consequently may result in energy savings. Hence, cyclohexane was chosen as the entrainer used in the azeotropic distillation.

4.6. Process Simulation. A tailored process for the recovery of dilute sulfuric acid from the titanium pigment industry is shown in Figure 9. The dilute sulfuric acid (20%) is first increased to 40% by direct evaporation, using the by-produced steam from the titanium dioxide industry as the heating source. The sulfuric acid is then enhanced by azeotropic distillation using cyclohexane as the entrainer to a concentration over 60%. The enriched sulfuric acid from the bottom of the distillation column is pumped to an evaporator to recover cyclohexane, and then sent for reuse. The overhead vapor from the distillation column is cooled and separated into two phases in the decanter. The upper organic phase, as well as makeup cyclohexane, is returned to the distillation column as reflux, while the water phase is sent to an evaporator to recover the cyclohexane in water.

Simulation of the above-described process was performed using Aspen Plus software with the private data bank established in this work,[33−35] and the simulation flowsheet for the whole process is shown in Figure 10. In this study, the RadFrac model in Aspen Plus, which can perform rigorous VLL three-phase calculations, was adopted to simulate the azeotropic distillation column. The column was designed as a packed column with 4 theoretical stages (including reboiler) without condenser. The inflow sulfuric acid and recycled cyclohexane are fed from the second and first stage,

dx.doi.org/10.1021/ie5013079 | Ind. Eng. Chem. Res. 2014, 53, 11794−11804

Table 8. Experimental Heterogeneous Azeotropic Distillation Operating Conditions to Enrich Dilute Sulfuric Acid from 20% to 60%

no.	entrainer	number of stages	input stage	input flow rate (mL/min)	heating power (kW)	bottom temperature (K)
1	cyclohexane	14	6	1.5	0.32	371.9
2	cyclohexane	14	6	0.65	0.23	368.1
3	octane	14	6	1.18	0.32	409.4
4	octane	14	6	0.87	0.23	410.5
5	cyclohexane	8	3	1.43	0.32	389.9
6	cyclohexane	8	3	1.11	0.23	385.5
7	octane	8	3	1.33	0.32	412.2
8	octane	8	3	0.69	0.23	409.3

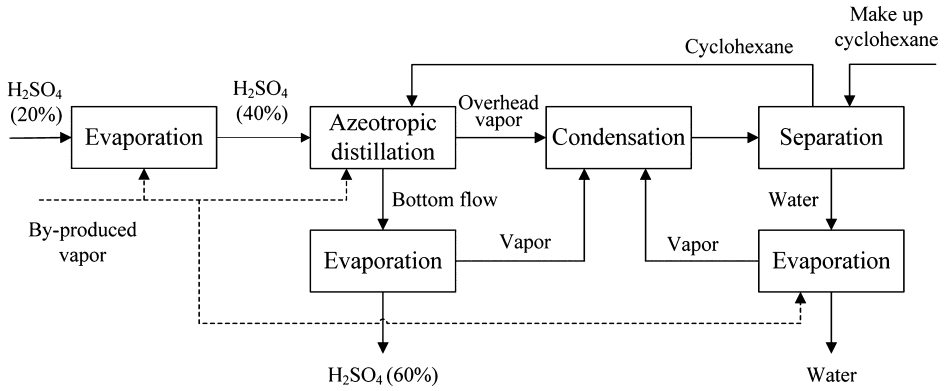

Figure 9. Flowsheet for the azeotropic distillation process for sulfuric acid recovery.

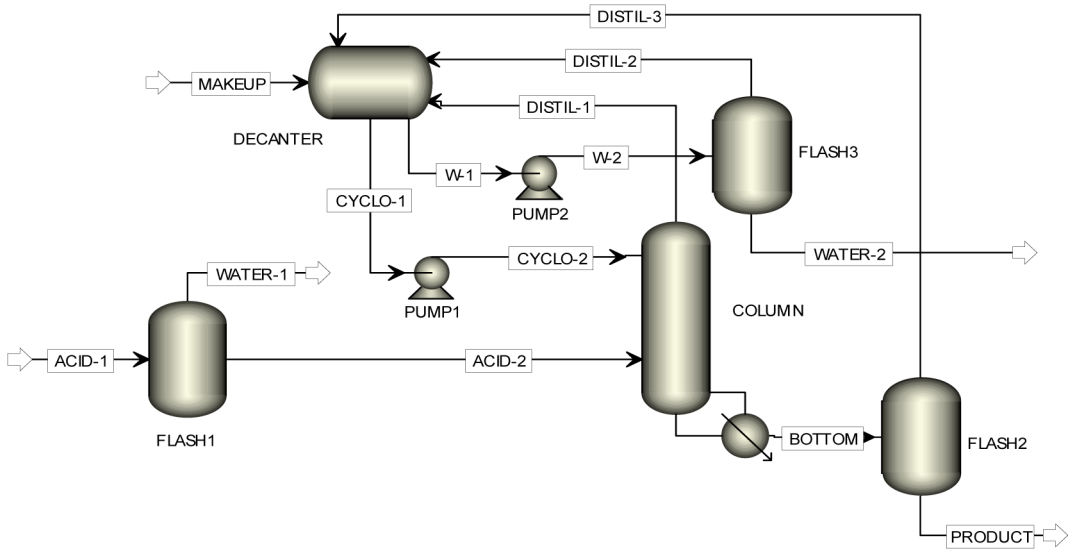

Figure 10. Simulation flowsheet of the azeotropic distillation process for sulfuric acid recovery.

respectively. The physical properties of the heterogeneous system are complex, so the convergence method entitled "Azeotropic", incorporated in Aspen, was selected for the distillation column.[36] A three-phase flash vessel model was chosen for the evaporator, and a two-phase liquid−liquid decanter model was selected for the decanter. The regressed parameters were used in the calculations for the distillation column, and the parameters from Aspen Plus LLE data bank were used in the calculations for the decanter.

According to a survey from Nanjing Titanium Dioxide Chemical Co., Ltd., a company in China with an annual production capacity of 50 000 tons of TiO_2 generates 340 thousand tons of dilute sulfuric acid annually. To recover all of the dilute acid, a total throughput of 40 000 kg/h is required for the process. The distillation column would have a feed rate of 20 000 kg/h, according to the sulfuric acid concentrations before and after evaporation. The simulation results show that the column, packed with Mellapak standard packing (250Y), would require a diameter of 4.56 m to meet the production demand. It can be seen from the stream results of the simulation, as tabulated in Table 9, that the dilute sulfuric acid can be successfully enriched from 20% to 68% by the azeotropic distillation process. The 68% sulfuric acid, which can be reused in the TiO_2 industry, is recovered at a flow rate of 11 806 kg/h, while the flow rate of makeup cyclohexane is only 2.267 kg/h. The temperature profile in the distillation column

dx.doi.org/10.1021/ie5013079 | Ind. Eng. Chem. Res. 2014, 53, 11794−11804

Table 9. Stream Results from the Azeotropic Distillation Process Simulation Based on Dilute Sulfuric Acid Feed Generated from a TiO_2 Company with an Annual Production Rate of 50 000 t

stream	ACID-1	ACID-2	MAKEUP	CYCLO-2	DISTIL-1	BOTTOM	PRODUCT	WATER-2
temperature (K)	343.2	392.3	313.2	333.2	348.9	360.55	424.76	375.08
pressure (bar)	1.3	1.3	1.1	1.2	1.1	1.3	1.1	1.1
total mole flow (kmol/h)	1857.8	743.14	0.0270	1742.7	2192.9	330.78	292.86	450.29
total mass flow (kg/h)	40000	19918	2.2670	146280	154390	14998	11806	8112.0
mass flow (kg/h)								
H_2SO_4	8000.0	8000.0	0	0	0	8000.0	8000.0	6.79×10^{-8}
H_2O	32000	11918	0	104.62	8216.7	3806.6	3806.4	8112.0
C_6H_{12}	0	0	2.2670	146175	146173	3190.7	0.002 57	0.001 22
mass fraction								
H_2SO_4	0.200	0.402	0.00		0	0.533	0.678	1.71×10^{-11}
H_2O	0.800	0.598	0.00	7.15×10^{-4}	0.053 22	0.254	0.322	1
C_6H_{12}	0	0	1	0.999 28	0.946 78	0.213	2.14×10^{-7}	1.53×10^{-7}

shown in Figure 11 demonstrates that the temperature at the bottom of the distillation column is only 361 K, which is far less

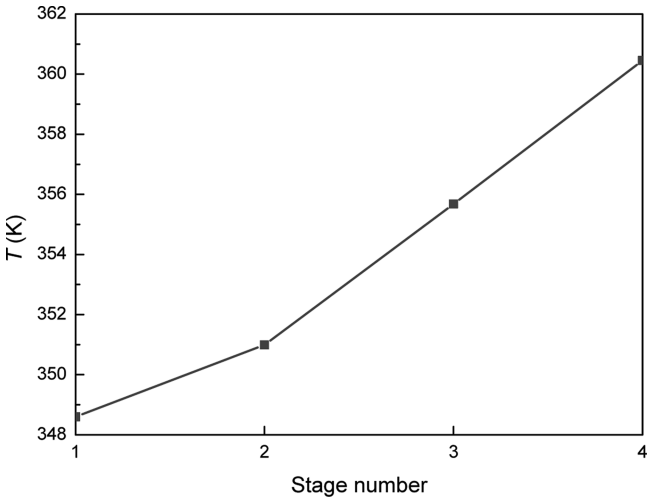

Figure 11. Temperature profile through the distillation column.

than the normal boiling point of sulfuric acid with a mass concentration of 68% (430 K). The sulfuric acid concentration profile in the water phase through the stages of the distillation column is illustrated in Figure 12. The mass fraction of sulfuric acid increases from 43% to 68% from stage 2 to 4 (counting from the top). The flow-rate profile in Figure 13 shows that a large amount of cyclohexane exists in the liquid phase in stages 1−3, but that its concentration is limited in the reboiler. The vapor flow rate increases with the increasing stage number.

5. CONCLUSIONS

A comprehensive thermodynamic model was established for the H_2SO_4 + $FeSO_4$ + H_2O + C_6H_{12} system on the basis of electrolyte NRTL model, and a private data bank was built by making use of new electrolyte NRTL parameters obtained via correlation of experimental VLE data for the $FeSO_4$ + H_2O and H_2SO_4 + $FeSO_4$ + H_2O systems and the azeotropic temperatures of H_2SO_4 + H_2O + entrainer (cyclohexane and octane) mixtures. Process simulation for the recovery of dilute sulfuric acid through heterogeneous azeotropic distillation using cyclohexane as the entrainer was successfully performed by Aspen Plus with the private data bank. The simulation results indicate that the dilute sulfuric acid can be enriched to

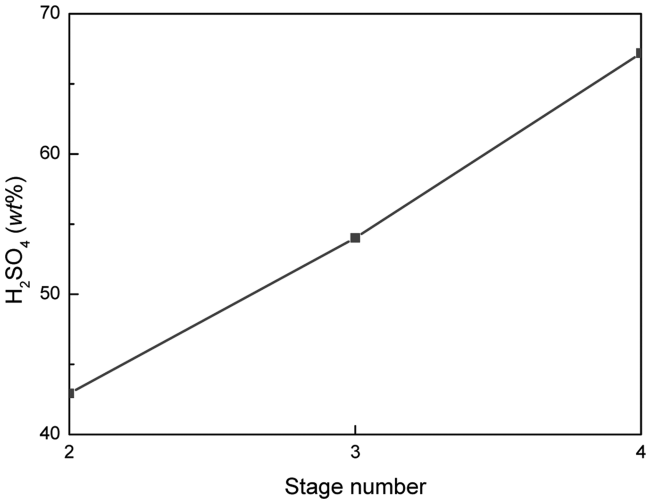

Figure 12. Sulfuric acid concentration profile in the distillation column.

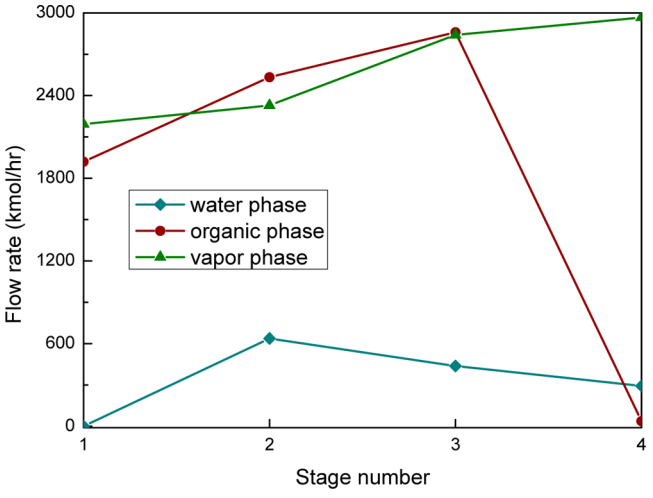

Figure 13. Flow rate profile through the distillation column.

68% by a packed column with only 4 theoretical stages. Distillation experiments also showed that this azeotropic distillation process can enhance dilute sulfuric acid to more than 60%. When cyclohexane is employed as the entrainer, a lower column bottom temperature of only 370 K is observed. For a company in China with an annual production capacity of

dx.doi.org/10.1021/ie5013079 | Ind. Eng. Chem. Res. 2014, 53, 11794−11804

50 000 tons of TiO_2, one packed column with a diameter of 4.56 m is required to recover all of the dilute sulfuric acid generated. This column, with a processing capacity of 20 000 kg/h, recovers the sulfuric acid (68%) at a flow rate of 11 800 kg/h. The experimental data, the model with new parameters, and the process simulation results provide knowledge necessary for the development of an industrial-scale process for the concentration and recovery of dilute sulfuric acid by azeotropic distillation.

■ ASSOCIATED CONTENT

Supporting Information

Antoine equation constants of the pure components; isobaric boiling points of the $FeSO_4$ (1) + H_2O (2) binary system; isobaric boiling points of the H_2SO_4 (1) + $FeSO_4$ (2) + H_2O (3) ternary system. This material is available free of charge via the Internet at http://pubs.acs.org.

■ AUTHOR INFORMATION

Corresponding Author

*Tel./fax: +86-10-62551557. E-mail: zhibaoli@home.ipe.ac.cn.

Notes

The authors declare no competing financial interest.

■ ACKNOWLEDGMENTS

The support of the National Basic Research Development Program of China (973 Program with Grant 2013CB632605) and the Science and Technology Planning Project of Qinghai Province (2012-G-213A) is gratefully acknowledged.

■ NOMENCLATURE

A = Debye−Hückel parameter
C = adjustable parameter of the electrolyte NRTL equation
D = adjustable parameter of the electrolyte NRTL equation
E = adjustable parameter of the electrolyte NRTL equation
G_m^E = molar excess Gibbs energy
I_x = ionic strength (mole fraction scale)
m = molality of species
M = molecular weight
n = data group
P = system pressure
P^S = saturated pressure of a pure component
Q_e = electron charge
r = Born radius
T^{ref} = reference temperature (273.15 K)
w_n = weight factor of a data group
x = liquid phase mole fraction
X = effective mole fraction of a species
y = vapor phase mole fraction
Z = charge number of an ion

Greek Letters

α = nonrandomness factor of the electrolyte NRTL equation
γ = liquid phase activity coefficient
ε_w = the dielectric constant of water
θ^s = Poynting pressure correction from P^S to P
ρ = "closest approach" parameter
σ = standard deviation
τ = energy parameter for the electrolyte NRTL equation
φ = vapor phase fugacity coefficient
φ^s = saturated vapor phase fugacity coefficient of a pure component

Subscripts and Superscripts

a = anion species
B = solvent
c = cation species
cal = calculated result
exp = experimental data
i = species
j = species
k = species
lc = local composition
NDG = number of data groups in the regression
S = saturated
z = feed composition
* = unsymmetrical reference state

■ REFERENCES

(1) Schuiling, R. D.; van Gaans, P. F. M. The waste sulfuric acid lake of the TiO_2-plant at Armyansk, Crimea, Ukraine. Part 1. Self-sealing as an environmental protection mechanism. *Appl. Geochem.* **1997**, *12*, 181−186.

(2) Kobe, K. A.; Fredrickson, R. E. Waste pickle liquor. Ferrous sulfate−sulfuric acid−water. *Ind. Eng. Chem. Eng. Data Series* **1956**, *1*, 13−17.

(3) Harris, T. R. Disposal of refinery waste sulfuric acid. *Ind. Eng. Chem.* **1958**, *50*, 81A−82A.

(4) Kuznetsova, A. S.; Sukharev, Y. G.; Litvinov, N. R. Treatment of acrylate production waste sulfuric acid. *Khim. Prom-st.* **1980**, *8*, 483−484.

(5) Song, K.; Meng, Q. Q.; Shu, F.; Ye, Z. F. Recovery of high purity sulfuric acid from the waste acid in toluene nitration process by rectification. *Chemosphere* **2013**, *90* (4), 1558−1562.

(6) Xu, J.; Fu, D.; Lu, S. G. The recovery of sulphuric acid from the waste anodic aluminum oxidation solution by diffusion dialysis. *Sep. Purif. Technol.* **2009**, *69* (2), 168−173.

(7) Hoak, R. D.; Lewis, C. J.; Hodge, W. W. Treatment of spent pickling liquors with limestone and lime. *Ind. Eng. Chem.* **1945**, *37*, 553−559.

(8) Colton, H. S. *Solid material from waste liquor*. U.S. Patent 2,165,344, July 11, 1939.

(9) Gunter, L.; Rudolf, G. *Process for the recovery of sulfuric acid.* Canada Patent CA 2,030,655, May 25, 1991.

(10) Bartholomew, F. J. Sulfuric acid recovery from waste liquors. *Ind. Eng. Chem.* **1952**, *44*, 541−545.

(11) Lawler, D. W.; Lyne, E. G. C. *Sulphuric acid recovery process.* EPO Patent EP 0421629, April 10, 1991.

(12) Stachera, D. M.; Childs, R. F.; Mika, A. M.; Dickson, J. M. Acid recovery using diffusion dialysis with poly(4-vinylpyridine)-filled microporous membranes. *J. Membr. Sci.* **1998**, *148*, 119−127.

(13) Li, G.; Li, Z.; Asselin, E. Determination and modeling of vapor−liquid equilibria for the sulfuric acid + water + butyl acetate + ethanol system. *Ind. Eng. Chem. Res.* **2013**, *52*, 3481−3489.

(14) Chien, I. L.; Zeng, K. L.; Chao, H. Y. Design and control of a complete heterogeneous azeotropic distillation column system. *Ind. Eng. Chem. Res.* **2004**, *43*, 2160−2174.

(15) Li, G.; Li, Z. Measurement and modeling of vapor−liquid equilibria for the octane + sulfuric acid + water + ethanol system. *J. Chem. Eng. Data* **2013**, *58*, 2044−2050.

(16) Clegg, S. L.; Brimblecombe, P. Application of a multicomponent thermodynamic model to activities and thermal properties of 0−40 mol·kg^{-1} aqueous sulfuric acid from <200 to 328 K. *J. Chem. Eng. Data* **1995**, *40*, 43−64.

(17) Pessoa, F. L. P.; Rasmussen, P.; Fredenslund, A. Calculation of vapour−liquid equilibria in water−sulfuric acid−sulfate systems using a revised extended UNIQUAC equation. *Lat. Am. Appl. Res.* **1992**, *22*, 195−206.

(18) Wang, P. M.; Anderko, A.; Young, R. D. A speciation-based model for mixed-solvent electrolyte systems. *Fluid Phase Equilib.* **2002**, *203*, 141−176.
(19) Chen, C. C.; Britt, H. I.; Boston, J. F.; Evans, L. B. Local composition model for excess Gibbs energy of electrolyte systems. Part I: Single solvent, single completely dissociated electrolyte systems. *AIChE J.* **1982**, *28*, 588−596.
(20) Chen, C. C.; Evans, L. B. A local composition model for the excess Gibbs energy of aqueous electrolyte systems. *AIChE J.* **1986**, *32*, 444−454.
(21) Chen, C. C.; Mathias, P. M. Applied thermodynamics for process modeling. *AIChE J.* **2002**, *48*, 194−200.
(22) Chen, C. C.; Song, Y. Generalized electrolyte-NRTL model for mixed-solvent electrolyte systems. *AIChE J.* **2004**, *50*, 1928−1941.
(23) Haghtalab, A.; Papangelakis, V. G.; Zhu, X. The electrolyte NRTL model and speciation approach as applied to multicomponent aqueous solutions of H_2SO_4, $Fe_2(SO_4)_3$, $MgSO_4$ and $Al_2(SO_4)_3$ at 230−270 °C. *Fluid Phase Equilib.* **2004**, *220*, 199−209.
(24) Que, H. L.; Song, Y. H.; Chen, C. C. Thermodynamic modeling of the sulfuric acid − water − sulfur trioxide system with the symmetric electrolyte NRTL model. *J. Chem. Eng. Data* **2011**, *56*, 963−977.
(25) Park, J.; Cho, J. H.; Jung, H.; Kumar, S.; Moon, I. Simulation and experimental study on the sulfuric acid decomposition process of SI cycle for hydrogen production. *Int. J. Hydrogen Energy* **2013**, *38* (14), 5507−5516.
(26) Li, G.; Li, Z. Determination and prediction of vapor−liquid equilibria for a system containing water + butyl acetate + cyclohexane + ethanol. *J. Chem. Eng. Data* **2012**, *57*, 2543−2548.
(27) Poling, B. E.; Prausnitz, J. M.; O'Connell, J. P. *The Properties of Gases and Liquids*, 5th ed.; McGraw-Hill: New York, 2001.
(28) Smith, J. M.; van Ness, H. C. *Introduction to Chemical Engineering Thermodynamics*; McGraw- Hill: New York, 1975.
(29) Aspentech. *Aspen Property System: Physical Property Methods and Models 11.1*; Aspen Technology, Inc.: Burlington, MA, 2001.
(30) Renon, H.; Prausnitz, J. M. Local compositions in thermodynamic excess functions for liquid mixtures. *AIChE J.* **1968**, *14*, 135−144.
(31) Pitzer, K. S. Electrolytes. From dilute solutions to fused salts. *J. Am. Chem. Soc.* **1980**, *102*, 2902−2906.
(32) Mock, B.; Evans, L. B.; Chen, C. C. Thermodynamic representation of phase equilibria of mixed-solvent electrolyte systems. *AIChE J.* **1986**, *32*, 1655−1664.
(33) Aspentech. *Aspen Plus 11.1 User Guide*; Aspen Technology, Inc.: Burlington, M.A., 2001.
(34) Luyben, W. L. *Distillation Design and Control Using Aspen Simulation*; John Wiley & Sons, Inc.: Hoboken, NJ, 2006.
(35) Luyben, W. L.; Chien, I. L. *Design and Control of Distillation Systems for Separating Azeotropes*; John Wiley & Sons, Inc.: Hoboken, NJ, 2010.
(36) Huang, X.; Zhong, W.; Du, W.; Qian, F. Thermodynamic analysis and process simulation of an industrial acetic acid dehydration system via heterogeneous azeotropic distillation. *Ind. Eng. Chem. Res.* **2013**, *52*, 2944−2957.